DOI: 10.26599/FSHW.2025.9250518

Contents lists available at SciOpen

Food Science and Human Wellness

journal homepage: https://www.sciopen.com/journal/2097-0765

China Food Publishing Co.

Anhydrosafflor yellow B ameliorates oxeiptosis and FUNDC1-mediated mitophagy through activation of mTOR signaling pathway in cerebral ischemia/reperfusion injury

Xian Zhang [a], Chongyu Shao [b], Weifeng Jin [a], Jingwei Li [a], Qiang Zeng [a], Tianhang Chen [b], Haitong Wan [b,*], Yu He [a,*]

[a] *School of Pharmaceutical Sciences, Zhejiang Chinese Medical University, Hangzhou, Zhejiang 310053, P.R. China.*

[b] *School of Basic Medicine Sciences, Zhejiang Chinese Medical University, Hangzhou, Zhejiang 310053, P.R. China.*

ABSTRACT: Anhydrosafflor yellow B (AHSYB) is an important water-soluble pigment in safflower, but its pharmacological research is quite sparse. In this study, we attempted to demonstrate the neuroprotective effect of AHSYB on oxeiptosis and FUNDC1-mediated mitophagy during cerebral ischemia/reperfusion injury (CI/RI) by establishing a classical middle cerebral artery occlusion/reperfusion (MCAO/R) rat model and an oxygen glucose deprivation/reperfusion (OGD/R) cellular model. The increase in apoptosis-inducing factor 1 (AIFM1) dephosphorylation level and the expression of autophagy marker, microtubule-associated proteins light chain 3 (LC3), confirmed the occurrence of oxeiptosis and mitophagy in ischemic stroke. AHSYB not only inhibited the expressions of kelch-like ECH-associated protein 1 (KEAP1) and phosphoglycerate mutase 5 (PGAM5), but also activated mammalian target of Rapamycin (mTOR) to repress the expressions of UNC-51-like kinase 1 (ULK1) and p- FUN14 domain containing 1 (FUNDC1) protein, and reversed CI/RI-induced mitochondrial structural abnormalities. Rapamycin, the mTOR inhibitor, obviously activated FUNDC1-mediated mitophagy and had a stimulative effect on the occurrence of oxeiptosis to some extent, which could be reversed by AHSYB. Our study suggested that AHSYB exhibited a noteworthy protective influence on MCAO/R rats and OGD/R-damaged SH-SY5Y cells, whose mechanism might be related to the inhibition of oxeiptosis and FUNDC1-mediated mitophagy. In addition, there seemed to be a certain relationship between the two modes of cell death, as inhibiting FUNDC1-mediated mitophagy with mTOR also appeared to ameliorate oxeiptosis. All these findings have implications for developing new therapeutic strategies for neurological diseases, providing important insights into the application of AHSYB in functional foods.

Keywords: Anhydrosafflor yellow B, cerebral ischemia/reperfusion injury, Oxeiptosis, FUNDC1-mediated mitophagy, mTOR signaling pathway

1. Introduction

Safflower is considered a versatile crop in the fields of agriculture, food, and medicine in both traditional and current research [1]. Safflower seed oil is regarded as a healthier vegetable oil with anti-hypercholesterolemia and antioxidant properties [2]. The red/yellow pigments extracted from safflower

***Corresponding author**
whtong@126.com (Haitong Wan), heyu0923@hotmail.com

Received 9 October 2024
Received in revised from 4 November 2024
Accepted 6 January 2025

are used to dye fabrics or as food additives to enhance attractiveness [3]. In the field of medicine, its therapeutic applications span a range of diverse ailments, encompassing cardiovascular and cerebrovascular diseases, blood stasis, and osteoporosis, and so on [1, 4]. The pharmacological effects of safflower primarily stem from safflower yellow [5, 6], and hydroxysafflower yellow A (HSYA) and dehydrated safflower yellow B (AHSYB) stand out as notable representatives [7]. HSYA has been officially recognized in the *Chinese Pharmacopoeia* as a key ingredient for quality control of safflower, and most pharmacological studies related to safflower were mainly focused on HSYA [3]. Despite AHSYB being the second most abundant active component, there is a scarcity of research exploring its pharmacological effects.

Reactive oxygen species (ROS) constitute a class of highly reactive oxidizing substances, and they are widely regarded as a harmful reactive particle due to its ability to deteriorate proteins, lipids, and nucleic acids within cells, and exacerbate cellular stress responses [8]. The intracellular ROS level is strictly controlled by multiple clearance systems to ensure timely regulation [9]. Globally, ischemic stroke resulting from the occlusion of cerebral arteries stands as a preeminent cause of chronic disability [10]. Oxidative stress activated by excessive ROS leads to cell damage and neuronal death, are essential in the pathogenesis of cerebral ischemia/reperfusion injury (CI/RI) [11]. The pivotal significance of clearing dysfunctional mitochondria and eliminating aberrant oxidative stress in the ischemic cascade has been confirmed [12], and mitochondria were also considered the primary targets for treating CI/RI [13, 14].

Oxeiptosis is a ROS-sensitive, caspase-independent, and non-inflammatory mode of cell death [15], whose essential prerequisite is high concentration of ROS, and decisive indicator is dephosphorylation of apoptosis-inducing factor 1 (AIFM1) [16]. Under external stimuli or pathological conditions, excessive ROS produced by cells induce the dissociation of Kelch ECH associating protein 1 (KEAP1)/phosphoglycerate mutase 5 (PGAM5) from the outer membrane of mitochondria. PGAM5 enters mitochondria and interacts with AIFM1, causing phosphorylation at Ser116 [16, 17]. The precise mechanisms underlying this novel cell death way in human diseases remain largely elusive, and no research in the field of CI/RI. It has been confirmed that oxidative stress, instigated by an excessive accumulation of ROS, arose during the process of ischemia/reperfusion (I/R) [18] , but still unknown whether excessive ROS led to oxeiptosis in the pathological process of CI/RI.

Mitophagy serves as a crucial mitochondrial quality control mechanism [19-21]. A modest amount of mitophagy helps maintain cellular homeostasis, but overactivated mitophagy results in a significant reduction in mitochondrial mass, inadequate energy production, and the exacerbation of cellular damage [13, 22, 23]. FUN14 domain-containing 1 (FUNDC1), a mammalian mitophagy receptor, primarily orchestrates ischemia-induced mitophagy through its interaction with microtubule-associated protein 1 light chain 3 (LC3). Prior studies on ischemic diseases outside the central nervous system have demonstrated that FUNDC1-mediated mitophagy adversely affects cellular survival and functionality during I/R [24]. The precise role of FUNDC1 in ischemia stroke pathogenesis remains underexplored [25]. Although PGAM5 is one of the characteristic proteins of oxeiptosis, it also plays an important regulatory role in other cell death

modes [26], participating in the dephosphorylation of FUNDC1 and promoting mitophagy [27, 28]. We hypothesize that with PGAM5 as the intersection, it seems to be some overlap between oxeiptosis and FUNDC1-mediated mitophagy.

Therefore, in this study, we attempted to demonstrate the occurrence of oxeiptosis and FUNDC1-mediated mitophagy during CI/RI by establishing a classical MCAO/R rat model and an OGD/R cellular model [29-31]. And we further investigated whether AHSYB intervened in these two cell death ways by activating mTOR to exert therapeutic effects against CI/RI, providing new treatment strategies for ischemic stroke.

2. Materials and methods

2.1 Drugs and reagents

AHSYB (purity > 98%) was prepared in Chemical Laboratory of traditional Chinese medicine (School of Pharmaceutical Sciences, Zhejiang Chinese Medical University). HSYA (purity > 98%, 78281-02-4) and Rapamycin (S17098) were acquired from Shanghai Yuanye Biotechnology Co., Ltd. (Shanghai, China). Edaravone (Eda, HY-B0099) was procured from MedChemExpress Biotechnology Co., Ltd. (Shanghai, China). The ROS, lactate dehydrogenase (LDH) and ATP enzyme-linked immunosorbent assay (ELISA) kits were obtained from Jiangsu Meibiao Biotechnology Co., Ltd. (Nanjing, China).

2.2 Molecular docking

AHSYB served as the ligand to dock mTOR protein to initially determine whether mTOR is one target of AHSYB. AHSYB (ID: 488229091) was saved as SDF format file from the Pubchem database (https://pubchem.ncbi.nlm.nih.gov). The 3D structure of mTOR was retrieved and downloaded as PDB format file from the protein database (ID: 7PED, https://www.rcsb.org) and the Uniport database (ID: P42346, https://www.uniprot.org). In the Autodock Vina software (version 1.2.5), we first purified the structure of mTOR protein by removing water molecules and original ligands, and further adding hydrogen and setting the docking pocket to facilitate the docking operation. Center x = 38.098, center y = 47.991, center z = 34.246, size x = 44.767, size y = 60.567, size z = 57.933, were applied to create the grid box in this study. The docking results were visually presented in Pymol software (version 2.4.0).

2.3 Experimental animals and MCAO/R model establishment

The experimental protocol was granted approval by the Animal Ethics and Welfare Committee of Zhejiang Chinese Medical University, ensuring that all experimental animals received compassionate care in accordance with the Guide for the Care and Use of Laboratory Animals. Adult male specific pathogen-free Sprague-Dawley rats (280-300 g) were sourced from Zhejiang Chinese Medical University Laboratory Animal Research Center and accommodated in a climate-controlled environment, maintaining a humidity level of (50 ± 5)% and a temperature of (22 ± 2) ℃.

The MCAO/R model was established utilizing the methodology described by Zea Longa [32]. The left common carotid artery (CCA), internal carotid artery (ICA), and external carotid artery (ECA) were carefully

dissociated and ligatures. A tiny incision was created in the CCA to allow for the insertion of a silicone-coated 4-0 nylon monofilament. This monofilament was subsequently advanced 18-19 mm into the middle cerebral artery for 1 h and slowly pulled to perform reperfusion. Notably, the sham group underwent identical surgical procedures, excluding the insertion of the nylon monofilament.

2.4 Administration of drugs

Experimental rats were randomly assigned to nine distinct groups: sham group, MCAO/R group, AHSYB (2, 4, and 8 mg/kg) groups, HSYA (4 mg/kg) group, Edaravone (Eda, 3 mg/kg) group, Rapamycin (3 mg/kg) group, and Rapamycin (3 mg/kg) + AHSYB (4 mg/kg) group, with eight rats in each group. The rats were weighed before daily administration, and the doses were calculated based on their weights. All drugs were dissolved in normal saline, with rapamycin administered before MCAO/R and all other drugs administered after MCAO/R. Rapamycin was administered intraperitoneally once daily for 3 consecutive days, and the other medications were injected intravenously through the tail daily for 3 days. Rats in the sham group and MCAO/R group received an equivalent volume of normal saline injected intravenously through the tail daily for 3 days as a control.

2.5 Neurological deficit score

The neurobehavioral deficits exhibited by the rats were quantitatively evaluated using the methodology described by Longa, and all groups were scored on a 5-point scale using a double-blind methodology. The first neurological deficit score was performed on the conscious rats after MCAO/R to evaluate whether the model was successfully established. After 3 days of administration, rats underwent the second neurological deficit score.

2.6 Examination of cerebral infarct volume

The brains were taken out expeditiously after execution, frozen, and sectioned into 2mm-thick coronal slices. Subsequently, these slices were immersed in a 2% 2,3,5-triphenyl tetrazolium chloride (TTC) solution maintained at 37℃ for 15 min. The normal brain tissue stained red, whereas the infarcted tissue appeared pale. High-resolution digital photography was employed to capture images of the brain slices, which were subsequently analyzed with Image J software to precisely determine the infarct volume.

2.7 Hematoxylin-Eosin (HE) Staining

Brain tissue was preserved in 4% paraformaldehyde (PFA), embedded in paraffin and cut into 5 μm coronal slices. Then the slices were deparaffinized and hydrated, and stained with HE. Lastly, the stained sections were securely sealed with neutral resin and observed under a microscope, utilizing both 200× and 400× magnifications.

2.8 SH-SY5Y cells OGD/R model establishment and treatment

The SH-SY5Y cells were maintained in DMEM/F12 medium supplemented with 15% FBS and 100 $\mu g \cdot mL^{-1}$ antibiotics (penicillin and streptomycin), cultured in a humidified incubator at 37℃. The

establishment of OGD/R model was same as the previous research [29]. Rapamycin was administered 1 h before the onset of OGD/R.

2.9 Cell viability assay

SH-SY5Y cells were subjected to various concentrations of AHSYB, HSYA, or Eda (10, 20, 40, 60, 80, 100, 120, 140, 160 μmol/L) after OGD 4 h. After 24 h of cultivation under normal conditions, replace the medicated medium with 100 μ L of serum-free medium containing 10% CCK-8 solution, and then incubate for 1 h at 37℃ in a no-light atmosphere. Subsequently, the absorbance of the cells was determined at 450 nm employing a microplate reader.

2.10 Measurement of intracellular ROS, ATP activities and LDH leakage

Rat serum samples were received by collecting blood from the aorta abdominalis and centrifuging at 4,000 r/min for 15 min. The SH-SY5Y cells were sonicated in an ice bath and fragmented, and centrifuged at 3,000 r/min for 10 min to collect the supernatant. All measurements were performed using the specific ELISA kits: ROS (Cat# MB-6608A), LDH (Cat# MB-6863A), and ATP (Cat# MB-6913A), strictly adhering to the manufacturer's instructions.

2.11 Transmission electron microscopy (TEM)

SH-SY5Y cells were fixed in 2.5% glutaraldehyde solution, treated with 1% osmic acid + 1.5% K_3 [Fe $(CN)_3$] for 1 h, post-fixed with TCH for 1 h, and then stained with 2% double oxygenic uranium overnight. Subsequently, gradient dehydration, embedding, and slicing were performed. Finally, the mitochondrial morphology and autophagic vesicles were inspected by transmission electron microscopy (JEOL, Peabody, MA).

2.12 Real-Time PCR assay of KEAP1, NRF2, PGAM5, AIFM1, mTOR, ULK1, FUNDC1 and LC3 mRNA levels

The total RNA was extracted from the ipsilateral hemisphere brain tissues of rats and SH-SY5Y cells utilizing the Trizol reagent. The procedure of RT-PCR was same as the previous research [3]. The primers of KEAP1, PGAM5, AIFM1, mTOR, ULK1, FUNDC1, and LC3 were synthesized by Sangon Biotech (Shanghai) Co., Ltd., and the sequences of these primers are presented in Tab. S1.

2.13 Western blot assay of KEAP1, PGAM5, AIFM1, p-AIFM1, mTOR, ULK1, p-FUNDC1 and LC3 protein expressions

Proteins were extracted from brain tissues and SH-SY5Y cells utilizing the RIPA Lysis Buffer. Subsequently, polyacrylamide gel electrophoresis was employed to separate the proteins, which were then electrophoretically transferred onto PVDF membranes. These membranes were blocked with 10% skim milk for 1 h, followed by incubation with primary antibodies overnight and secondary antibodies for 2 h. and exposed to Enhanced Chemiluminescence reagent for develop. Image J software was utilized to quantitatively analyze the relative density of protein bands.

2.14 Statistical analysis

The results were presented as the mean ± SD. SPSS software (version 26.0) and GraphPad Prism software (version 6.0) were used to analyze and plot the obtained data. The significance of differences was rigorously examined using one-way ANOVA, followed by the LSD test, and considered statistically significant at P values of < 0.05.

3. Results

3.1 Molecular docking of AHSYB with mTOR protein

We performed molecular docking between AHSYB and the mTOR protein to determine the binding posture and interaction between the drug and the target using Autodock Vina software (version 1.2.5). Ligands stably integrated with protein when the binding affinity value was below -5 kcal/mol, and the molecular docking results showed that AHSYB and the mTOR protein have a very stable interaction with a low binding energy of -10.6 kcal/mol (Figure 1).

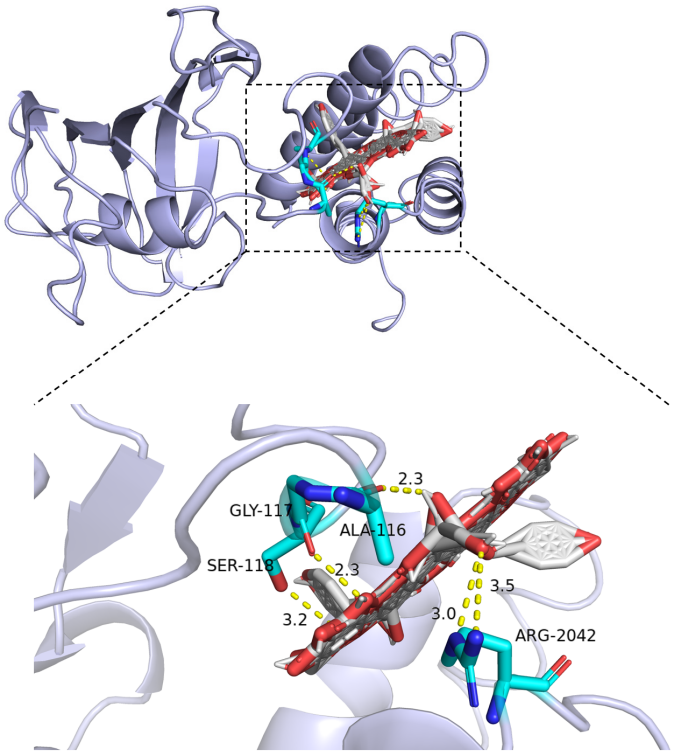

Figure 1. The results of molecular docking of AHSYB with mTOR (3D interaction structure)

3.2 AHSYB reduced the neuronal damage after MCAO/R

The results of TTC staining (Figure 2B, 2C) revealed in the sham group, the entire brain of the rat exhibited uniform red staining, confirming the absence of any infarct region. Contrastingly, in the MCAO/R rats, approximately half of the brain appeared pale after staining. The infarct volumes observed in the AHSYB groups were significantly reduced in comparison to those in the MCAO/R group. The results of neurological deficit scores (Figure 2D) presented no neurobehavioral deficits were detectable in the sham group. The MCAO/R group showed significant neurobehavioral deficits, with rats collapsing to the left during rest and circling to the left during crawling. Compared with the MCAO/R group, AHSYB significantly improved the neurological impairment of MCAO/R rats.

HE staining (Figure 2E) demonstrated the absence of apparent pathological alterations in the sham group. But in the MCAO/R group, the distinct pathological changes were observed, characterized by loosely arranged pyramidal cells, severely pyknotic or absent cell nuclei, and the presence of enlarged vacuolar structures. AHSYB ameliorated these pathological alterations, with a reduction in vacuolar structures, suggesting a significant attenuation of the MCAO/R-induced injury. Collectively, the results of HE staining were consistent with TTC staining and neurological deficit scores, jointly suggested that AHSYB had a significant neuroprotective effect in MCAO/R rats.

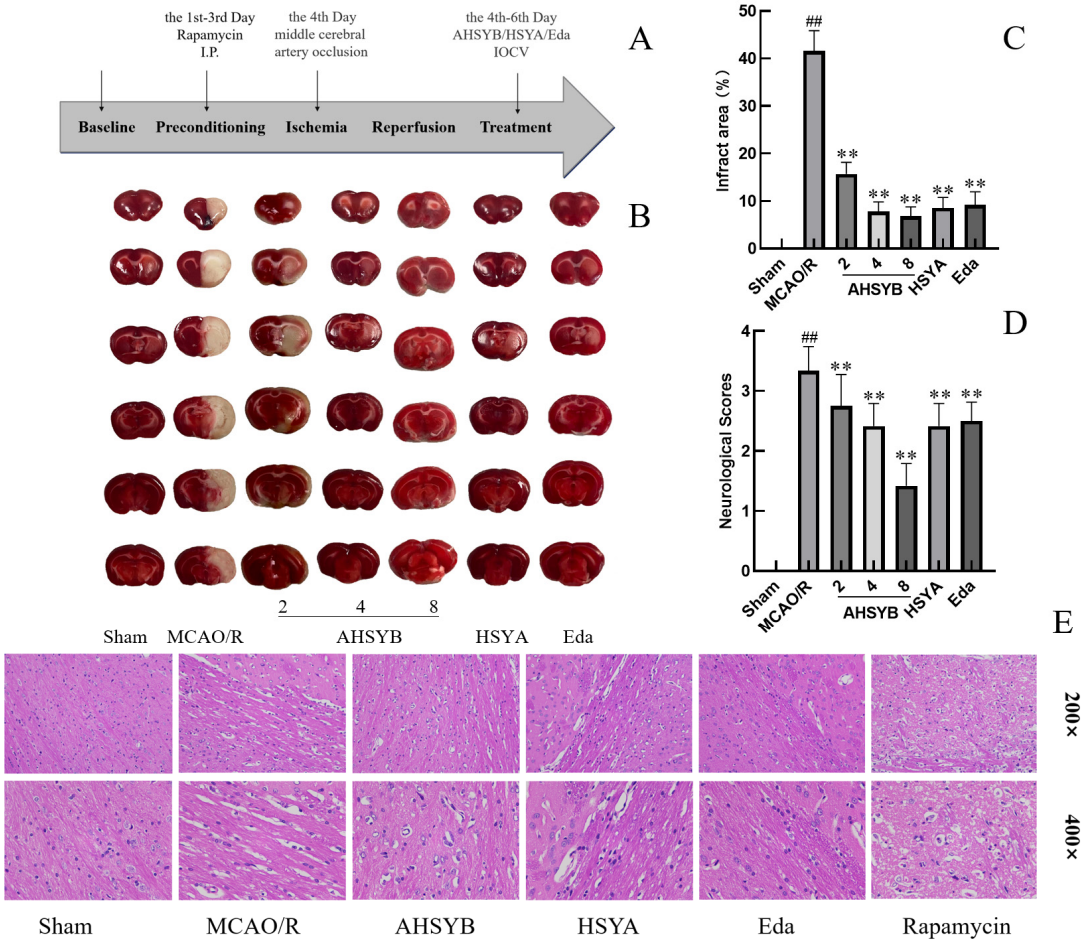

Figure 2. AHSYB reduced the neuronal damage in MCAO/R rat brain. (A) Schematic illustration of the experimental protocol; (B) Chemical structure of AHSYB; (C) Representative images of TTC staining; (D) The percentage of cerebral infarction volume in the same hemisphere; (E) Neurological deficit score; (F) Photomicrographs of HE-stained tissue (magnification = 200× and 400×). Data were shown as the mean ± SD; n=6. $^{\#\#}P < 0.01$ vs. the sham group; $^{**}P < 0.01$ vs. the MCAO/R group; $^{\$\$}P < 0.01$ vs. the Rapamycin group

3.3 AHSYB protected MCAO/R rats from ROS-induced oxeiptosis

It is worth noting that serine at position 116 of AIFM1 is highly conserved, and its dephosphorylation (serine → alanine) marks the occurrence of oxeiptosis, and high concentration of ROS is an essential prerequisite for cell oxeiptosis. The Western blot results of MCAO/R group showed that AIFM1 was significantly dephosphorylated, and the ROS content significantly increased, compared with the sham group (Figure 3A, 3I). In addition, the MCAO/R group exhibited a decline in LDH release and ATP production, aligning with prior reports about oxeiptosis [15]. These observations suggested the occurrence of oxeiptosis in

brain tissues during ischemic stroke. AHSYB treatment effectively reduced ROS accumulation in the injured brain tissues (Figure 3A), markedly reduced the level of AIFM1 dephosphorylation, and normalized LDH release and ATP production (Figure 3B, 3C). These findings indicated that AHSYB might play a protective role in ischemic stroke by mitigating oxeiptosis and oxidative stress.

3.4 AHSYB intervened KEAP1 and PGAM5 expressions to repress oxeiptosis

The dissociation of PGAM5 from KEAP1 initiates the downstream events leading to cell death. We observed a significant downregulation of KEAP1, concomitant with an upregulation of PGAM5 upon the establishment of the MCAO/R model. And AHSYB resulted in a reversal in the expressions of KEAP1 and PGAM5 (Figure 3E, 3F, 3G, 3H), suggesting a modulatory role of AHSYB in oxeiptosis. We speculated that AHSYB intervention effectively depleted PGAM5, rescuing MCAO/R rats from oxeiptosis.

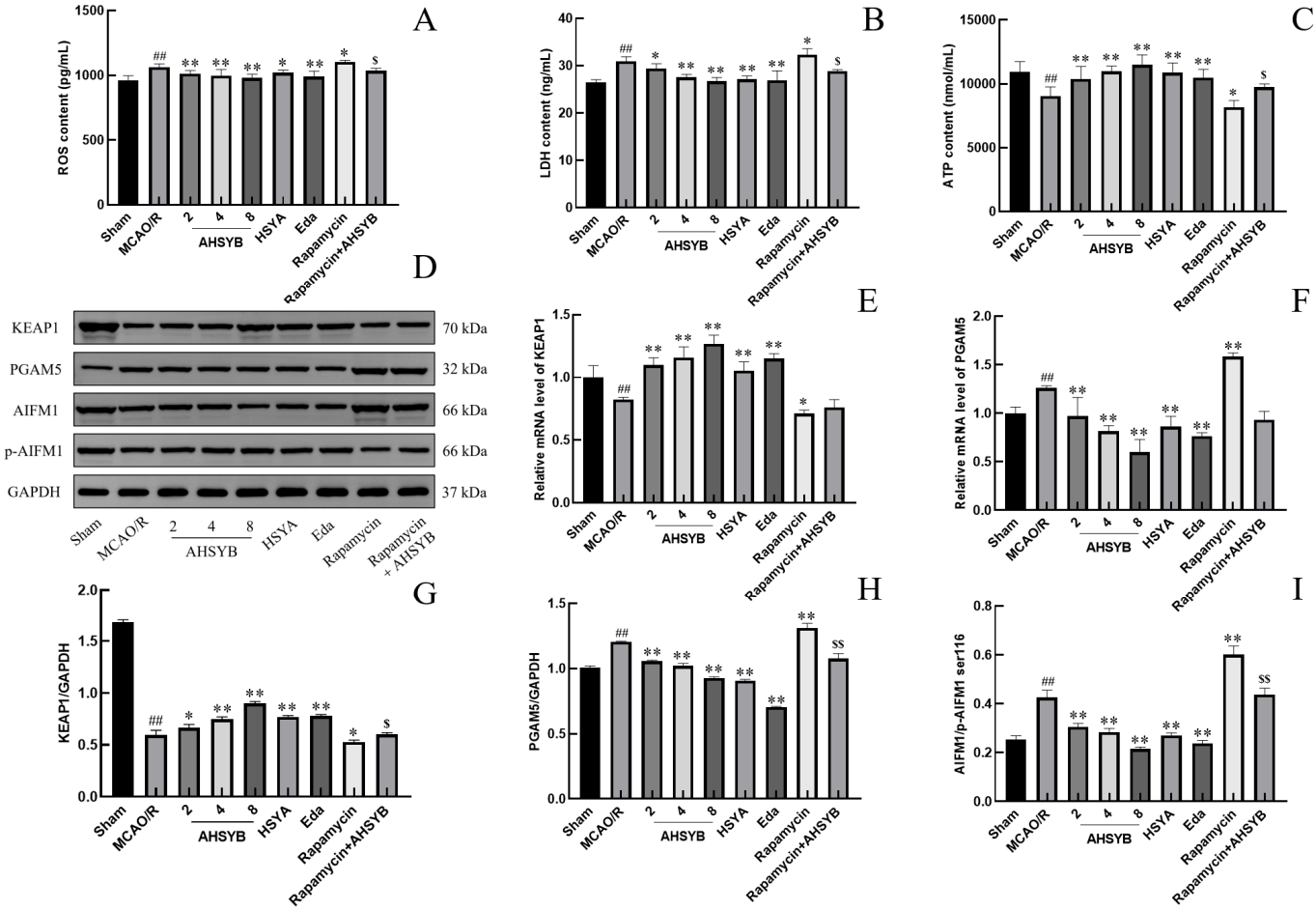

Figure 3. AHSYB protected MCAO/R rats from ROS-induced oxeiptosis. Effects of AHSYB on (A) ROS, (B) LDH and (C) ATP in CI/RI rat serum; (D) Representative images of the expression of proteins; The mRNA expression level of (E) KEAP1 and (F) PGAM5; The protein expression level of (G) KEAP1 and (H) PGAM5; (I) The ratio of AIFM1/p-AIFM1; Data were shown as the mean ± SD; n=3. $^{\#\#}P < 0.01$ vs. the Sham group; $^{*}P < 0.05$ vs. the MCAO/R group, $^{**}P < 0.01$ vs. the MCAO/R group; $^{\$}P < 0.05$ vs. the Rapamycin group, $^{\$\$}P < 0.01$ vs. the Rapamycin group

3.5 AHSYB alleviated excessive mitophagy caused by cerebral ischemia/reperfusion

The marked increase in the LC3-II/LC3-I ratio in brain tissue specimens from MCAO/R rats compared to those from sham rats (Figure 4I), suggesting that CI/RI induced mitophagy. Compared to the sham group, the

MCAO/R group exhibited a reduction in mTOR expression levels, concomitant with an elevation in ULK1 and FUNDC1 expression. AHSYB significantly upregulated mTOR expression levels, while concurrently downregulating ULK1 and FUNDC1 expression levels in comparison to the MCAO/R group (Figure 4G, 4H). In contrast, the mTOR expression in the Rapamycin group was much lower than that of the MCAO/R group (Figure 4F), and the expression of ULK1, FUNDC1, and LC3 was significantly increased. But additional AHSYB treatment led to a substantial decrease in the expressions of proteins associated with autophagy. These results suggested that AHSYB potentially attenuated CI/RI-triggered mitophagy by modulating the mTORC1-ULK1-FUNDC1 signaling cascade.

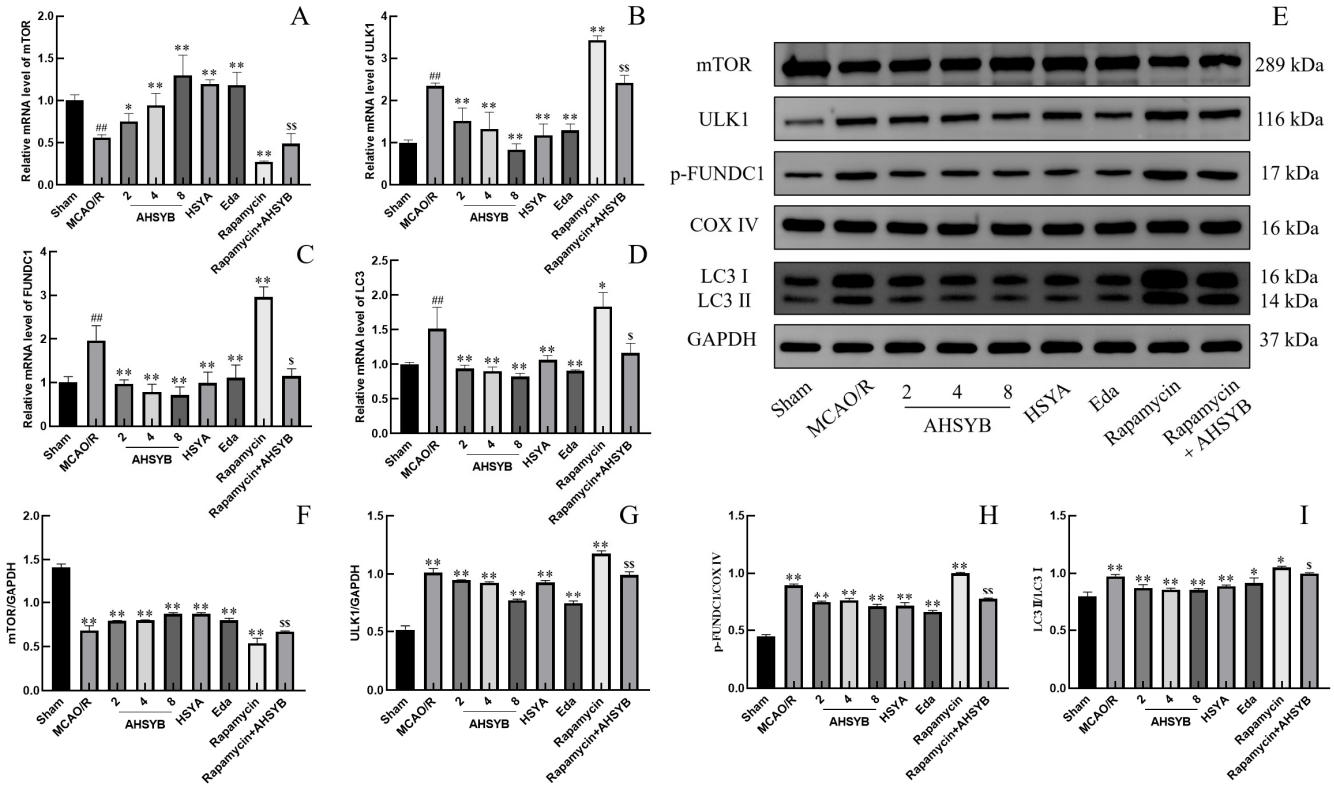

Figure 4. AHSYB alleviated excessive mitophagy caused by cerebral ischemia/reperfusion *in vivo*. The relative mRNA levels of (A) mTOR, (B) ULK1, (C) FUNDC1, and (D) LC3; (E) Representative images of the expression of proteins; The protein expression level of (F) mTOR, (G) ULK1, (H) p-FUNDC1, and (I) LC3; Data were shown as the mean ± SD; n=3. $^{\#\#}P < 0.01$ vs. the Sham group; $^{*}P < 0.05$ vs. the MCAO/R group, $^{**}P < 0.01$ vs. the MCAO/R group; $^{\$}P < 0.05$ vs. the Rapamycin group, $^{\$\$}P < 0.01$ vs. the Rapamycin group

3.6 AHSYB improved OGD/R-induced SH-SY5Y cell damage and oxidative stress

We assessed the cytotoxic effects of AHSYB on SH-SY5Y cells to ascertain the proper concentration. AHSYB did not exhibit any impact on the viability of SH-SY5Y cells within the concentration range of 2.5 μmol/L to 160 μmol/L. Once the concentration of AHSYB surpassed 160 μmol/L, a decline in cell viability was observed (Figure S1). Subsequently, we tested the cell viability of OGD/R-injured SH-SY5Y cells treated with various concentrations of drugs. The OGD/R treatment suppressed cell viability, yet HSYA, AHSYB, and Eda significantly alleviated this impairment (Figure S1), which was consistent with previous research [33,

34]. Ultimately, the three selected concentrations of AHSYB were 40, 60, and 80 μmol/L, respectively. The concentration of HSYA was set to 60 μmol/L, and that of Eda was given a concentration of 80 μmol/L.

The OGD/R treatment enhanced ROS production, LDH release and subdued ATP level in SH-SY5Y cells (Figure 5A, 5B, 5C). AHSYB attenuated the levels of ROS and LDH in a dose-responsive manner, whereas concurrently augmented the concentrations of ATP. The observations indicated that AHSYB potently mitigated the oxidative stress triggered by OGD/R. And there was no statistically significant variation between HSYA, 60 μmol/L AHSYB, and Eda groups. Furthermore, Rapamycin exacerbated the impairment of cell viability and oxidative stress.

3.7 AHSYB treatment improved mitochondrial morphological changes and autophagy

The SH-SY5Y cells in the control group arranged closely, intercellular space was small. However, the number of cells in the vehicle group significantly decreased, cell body shrinkage and roundness, and increased intercellular space (Figure S2). We randomly selected the field of view within each group for cell counting. After exposure to OGD/R injury, the number of SH-SY5Y cells was significantly reduced compared to the control group (Figure 5E). AHSYB was able to improve the reduction of SH-SY5Y cell count after OGD/R treatment, restored abnormal changes in cell morphology. Simultaneously, we assessed the cell viability of each group, and in line with the above results, AHSYB significantly reversed the damage to cell viability (Figure 5D), exhibiting a noteworthy neuroprotective effect.

We further observed the morphological changes of mitochondria and autophagic vesicles using transmission electron microscopy. The mitochondria in the control group were oval and elongated in shape, with smooth outer membrane and the arrangement of the cristae was regular, but mitochondria in the vehicle group were in a shrunken or swollen state, with disrupted or significantly reduced cristae, indicating severe and irreversible damage to cells. AHSYB distinctly ameliorated mitochondrial aberrations and decreased the quantity of autophagic vesicles. The cells treated with Rapamycin displayed apparent mitochondrial abnormalities (Figure 5F), including swelling, vacuolization, irregular or broken inner membranes and cristae, and autophagic vesicles, whose aberrant phenomenon appeared to be more severe than the vehicle cells.

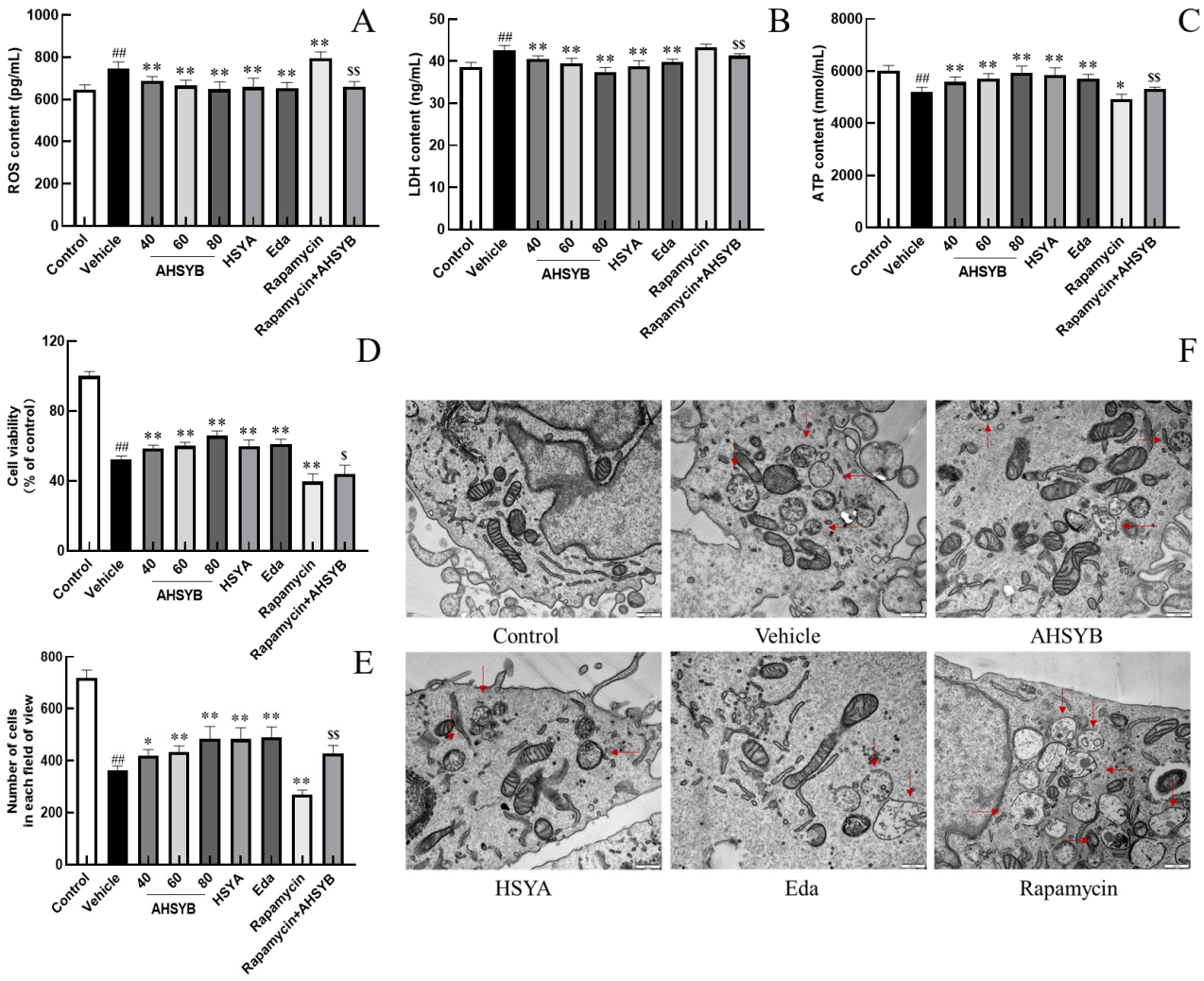

Figure 5. Protective effects of different concentrations of AHSYB on SH-SY5Y cells. Effects of AHSYB on (A) ROS, (B) LDH and (C) ATP on SH-SY5Y cells damaged by OGD/R; Effect of different drugs on (D) cell survival rate and (E) cell number in random field of view in each group; (F)Transmission electron microscopy representative images of the SH-SY5Y cells mitochondrial ultrastructure (Scale bars: 500 nm, the red arrows indicate autophagic vesicles). Data were shown as the mean ± SD; n=6. $^{\#\#}P < 0.01$ vs. the control group; $^{*}P < 0.05$ vs. the vehicle group, $^{**}P < 0.01$ vs. the vehicle group; $^{\$}P < 0.05$ vs. the Rapamycin group, $^{\$\$}P < 0.01$ vs. the Rapamycin group

3.8 AHSYB alleviated OGD/R-induced oxeiptosis induced by intervention of mTOR pathway

We have demonstrated that excessive mitophagy and oxeiptosis did occur during CI/RI *in vivo*. It seems to be an inseparable relationship between these two pathways. Therefore, we attempted to intervene in mTOR to explore the relationship between excessive mitophagy and oxeiptosis. After administration of Rapamycin, both the expression level of PGAM5 and the dephosphorylation level of AIFM1increased ($P < 0.01$, Figure 6), exacerbating cell oxeiptosis. But this excessive autophagy situation seemed to have significantly improved after administered AHSYB, possibly by restoring the expression of mTOR and its downstream proteins.

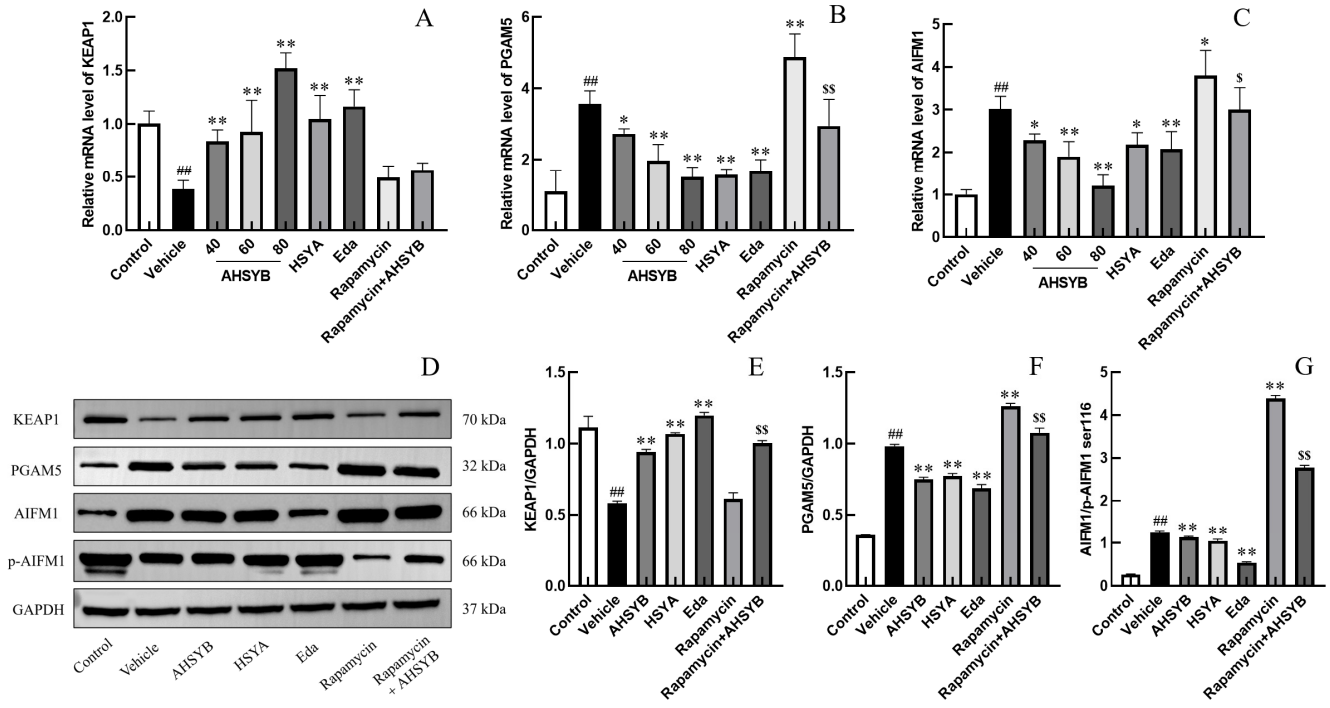

Figure 6. AHSYB alleviated oxeiptosis caused by cerebral ischemia/reperfusion *in vitro*. The relative mRNA levels of (A) KEAP1, (B) PGAM5, and (C) AIFM1; (D) Representative images of the expression of proteins; The protein expression level of (E) KEAP1, (F) PGAM5, and (G) AIFM1. Data were shown as the mean ± SD; n=3. $^{\#\#}P < 0.01$ vs. the control group; $^{*}P < 0.05$ vs. the vehicle group, $^{**}P < 0.01$ vs. the vehicle group; $^{\$}P < 0.05$ vs. the Rapamycin group, $^{\$\$}P < 0.01$ vs. the Rapamycin group

3.9 AHSYB improved OGD/R-induced excessive mitophagy

In comparison to the control group, the mTOR level in the vehicle group exhibited a marked reduction, and a significant elevation in the expressions of ULK1, FUNDC1, and LC3 ($P < 0.01$). After administering Rapamycin, the expression level of mTOR was extremely low, and the levels of mitophagy related genes ULK1, p-FUNDC1, and LC3 were significantly increased (Figure 7), indicating that Rapamycin inhibited the mTOR-ULK1-FUNDC1 pathway and exacerbated mitophagy. AHSYB gradually recovered the levels of ULK1, FUNDC1, and LC3, indicating that AHSYB partially antagonized the inhibitory effect of Rapamycin on mTOR, thereby exerting a protective effect on SH-SY5Y cells injured by OGD/R.

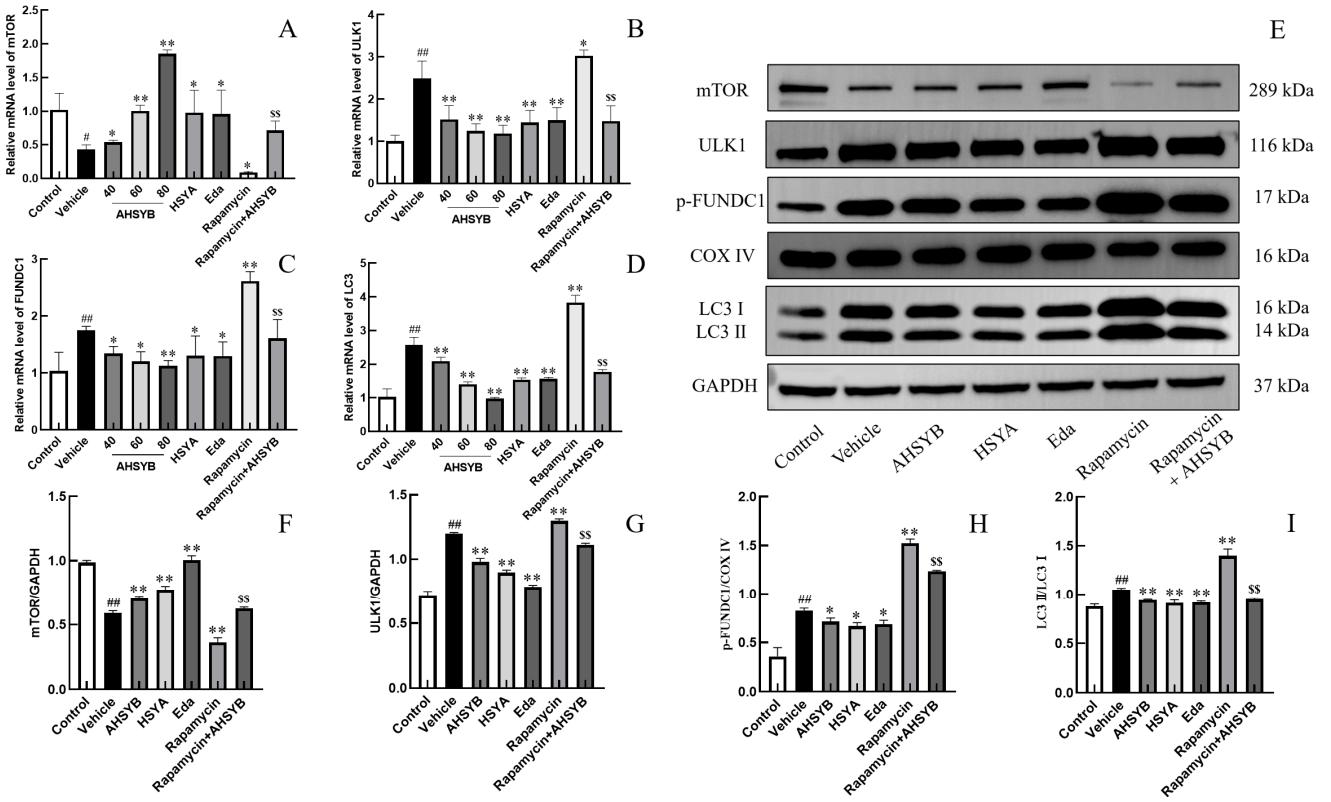

Figure 7. AHSYB alleviated excessive mitophagy caused by cerebral ischemia/reperfusion *in vitro*. The relative mRNA levels of (A) mTOR, (B) ULK1, (C) FUNDC1, and (D) LC3; (E) Representative images of the expression of proteins; The protein expression level of (F) mTOR, (G) ULK1, (H) p-FUNDC1, and (I) LC3. Data were shown as the mean ± SD; n=3. $^{\#}P < 0.05$ vs. the control group, $^{\#\#}P < 0.01$ vs. the control group; $^{*}P < 0.05$ vs. the vehicle group, $^{**}P < 0.01$ vs. the vehicle group; $^{\$}P < 0.05$ vs. the Rapamycin group, $^{\$\$}P < 0.01$ vs. the Rapamycin group

4. Discussion

The pathophysiological mechanisms of stroke have been extensively studied [10], sparking growing interest in the distinctive therapeutic benefits of traditional Chinese medicine [35]. Contrary to the single-target therapeutic approach of chemical drugs, natural medicine harnessed the synergistic effects of various components and biological pathways to facilitate the restoration of bodily homeostasis [36, 37]. Safflower yellow, a primary active component within safflower, exhibits notable antioxidative and neuroprotective properties [38]. Prior investigations have primarily centered on the pharmacological effect of HSYA, revealing its significant therapeutic potential in the management of cardiovascular and cerebrovascular diseases [39]. However, there is a growing recognition of AHSYB as a significant constituent of safflower, even though its neuroprotective mechanisms remain incompletely elucidated.

It was reported that dephosphorylated S116 on AIFM1 serves as a marker of oxeiptosis [16]. And in our experiment, significant mutation (dephosphorylation) was observed at position 116 of AIFM1, which was the direct evidence of oxeiptosis occurring in ischemic stroke. Oxeiptosis encompasses KEAP1-PGAM5-AIFM1 and is activated by detrimental levels of ROS [15]. ROS are indeed produced after cerebral ischemia/reperfusion, and we speculate that the accumulation of ROS during this pathological process has reached an excess that is sufficient to induce oxeiptosis. The ROS levels of male C57 mice were increased by

nearly 1.7 times after 1 h of middle cerebral artery occlusion and 24 h of reperfusion [40]. However, our experiment determined ROS in rat serum after 3 days and there was already some degree of self-recovery in cerebral ischemia/reperfusion-damaged rats. Thus, the measured ROS did not indicate a substantial excess, which was also a limitation of our paper.

The enhanced dephosphorylation of AIFM1, accompanied with upregulated expression of FUNDC1 and LC3 *in vivo* experiment, provided confirmation of oxeiptosis and FUNDC1-mediated mitophagy in ischemic stroke. After a 3-day treatment with AHSYB, the MCAO/R rats exhibited significant therapeutic effect in neurologic impairment, and marked reduction in oxidative stress. Furthermore, the expressions of FUNDC1 and LC3 were downregulated, and the levels of oxeiptosis indicators PGAM5 and AIFM1 were also notably reduced. These findings suggested that oxeiptosis and mitophagy in ischemic stroke were observably suppressed by AHSYB. The SH-SY5Y cells exposured to OGD/R resulted in the upregulated expressions of autophagy-related proteins ULK1, FUNDC1, and LC3, accompanied by a remarkable increase in autophagic vesicles. Furthermore, the critical indicators of oxeiptosis, PGAM5 and AIFM1, exhibited abnormal elevations. The results indicated that excessive mitophagy and oxeiptosis occurred in OGD/R-injured SH-SY5Y cells, which exacerbated cell damage and might be important participants in the pathogenesis of CI/RI.

Ischemic stroke leads to the destruction of the blood-brain barrier (BBB) twice. The first wave of BBB disruption is caused by a sudden interruption of cerebral blood flow which may quickly result in metabolic disturbances, inflammation, oxidative stress, neuronal death, degradation of tight junction proteins in BECs, BBB disruption, and increased BBB permeability, while the second wave occurs during blood reperfusion in ischemic areas, putting oxidative stress injury [41]. Because of the breakdown of BBB after ischemic stroke, medicines enter the brain via the bloodstream and exert therapeutic effects. AHSYB suppressed the expression of KEAP1, PGAM5, and AIFM1 in OGD/R-injured SH-SY5Y cells. Concurrently, AHSYB activated mTOR and reversed the deregulated expression of ULK1, p-FUNDC1, LC3, and evidently decreased the formation of autophagic vesicles. This supported the potential therapeutic role of AHSYB in ischemic stroke and further corroborated the findings of our in vivo investigations.

ROS play a diverse role in several cell death processes, and their threshold levels govern the activation of distinct cell death programs. The intracellular ROS concentration also serves as a critical determinant in modulating the interaction between KEAP1 and PGAM5. Low ROS level maintains the integrity of the KEAP1-NRF2-PGAM5 tripartite complex, and NRF2 regulates the expression of genes that protect cells. However, under severe stress conditions, high ROS levels disrupt the interaction between KEAP1 and PGAM5, thereby inhibiting the degradation of PGAM5 and leading to its accumulation and triggering a programmed cell death response. Literature reports have indicated that when exercise intensity reached a high level in an ozone environment, oxidative stress in myocardial tissue gradually intensified in myocardial tissue, and the Keap1-PGAM5-p-AIFM1-mediated "oxeiptosis" pathway was activated. However, the significance of oxeiptosis in pathological cell death in human diseases remains largely elusive, necessitating future

research to delve deeper into its role in various biological processes. To our knowledge, it is our first demonstration that oxeiptosis indeed occurs in CI/RI, evidenced by the dephosphorylation expression of p-AIFM1. This novel form of cell death holds significant implications for understanding the pathological mechanisms underlying stroke and potential therapeutic strategies.

Moreover, ROS initiate a range of cellular responses, including the activation of mitochondrial fission and autophagy to optimize the clearance of dysfunctional mitochondria [28]. At the fundamental level, mitophagy serves as an inevitable response necessary for maintaining normal biological and physiological activities. During mitochondrial stress, receptors situated on the outer mitochondrial membrane undergo augmented interactions with LC3 or other autophagy-related genes, thereby initiating mitophagy. In conditions of severe hypoxia and ischemia, mitophagy becomes overstimulated, leading to an overload of the autophagy system and the activation of apoptosis-related regulatory proteins. Existing literature has corroborated that cardiac I/R injury significantly increased the level of mitophagy and mitochondrial damage [42]. MTOR is widely recognized as a central controller of cell growth and a key suppressor of autophagy [43], primarily due to its interaction with ULK1 to restrain its activity and prevent the maturation of the autophagosome precursor structure. Following ischemic stroke, autophagy is triggered in brain cells exposed to the deprivation risk of oxygen and nutrient, stimulating autophagy either by directly activating ULK complexes through phosphorylation of Ser 317 and Ser 777 or indirectly by suppressing mTOR activity. Upon mitochondrial damage, FUNDC1 recruits ULK1 to the mitochondrial outer membrane, triggering mitophagy. Prior investigations have suggested that the activations of ULK1 and FUNDC1 might play a crucial regulatory role in CI/RI-induced autophagy [44], a notion that aligns with our experimental results.

In the previous investigation, we observed that AHSYB manifested protection against CI/RI by mitigating oxidative stress and apoptosis via the silent information regulator 1 (SIRT1) signaling pathway [30]. However, the question remains whether AHSYB suppresses FUNDC1-mediated mitophagy through the activation of the mTOR/ULK1 signaling pathway, which has yet to be reported. Consistent with previous reports of electroacupuncture treatment at Quchi and Zusanli [44, 45], AHSYB reduced neuronal autophagy by suppressing the elevation of LC3-II/I ratio and FUNDC1-mediated mitophagy related protein expressions, thereby conferring protection against CI/RI. In order to investigate the expression of mTOR-related signaling pathways in mitigating CI/RI, we additionally set up Rapamycin and Rapamycin + AHSYB groups. Administration of Rapamycin significantly elevated the protein ratio of LC3II/LC3I and augmented the number of autophagy vesicles, indicating its forceful stimulatory effect on autophagy. Rapamycin potentiated the expression of autophagy-associated proteins such as ULK1, p-FUNDC1, and LC3. Simultaneously, Rapamycin leaded to an elevation in the expression of PGAM5 and AIFM1 proteins and intensified cellular damage. However, AHSYB treatment abrogated the stimulatory effect of Rapamycin on autophagy, and suppressed CI/RI-triggered mitophagy by activating the mTOR signaling cascades. In contrast to Rapamycin group, the Rapamycin + AHSYB group exhibited reduced cellular death and a lower AIFM1/p-AIFM1 ratio. AHSYB exerted a protective effect on MCAO/R rats and SH-SY5Y cells subjected to OGD/R injury,

counteracting the suppressive effect of Rapamycin on mTOR. This further supported the moderation effect of AHSYB in mitophagy inhibition, and its ability to mitigate oxeiptosis to a certain extent.

5. Conclusion

Our experiment revealed elevated levels of oxeiptosis and FUNDC1-mediated mitophagy-related proteins in both MCAO/R rats and OGD/R-induced SH-SY5Y cells, and validated confirmed the occurrence of oxeiptosis and mitophagy in ischemic stroke. AHSYB, a bioactive component derived from the chalcones in safflower, safeguarded neurons against CI/RI both *in vivo* and *in vitro*, which effectively attenuated excessive FUNDC1-mediated mitophagy by modulating mTOR and ameliorate the occurrence of oxeiptosis. These results underscored the potential of AHSYB in countering CI/RI through its intervention in oxeiptosis and FUNDC1-mediated mitophagy, offering novel therapeutic strategies for neurological disorders, including ischemic stroke.

Ethics declaration

The animal experiments were performed by following the guidelines by the Institutional Animal Care and Use Committee of the Zhejiang Chinese Medical University (Laboratory Animal Certificate: 202208-0630) to minimize experiment-induced pain, suffering, and distress in rats.

Acknowledgments

This work was supported by the National Natural Science Foundation of China (No. 82374326).

Competing Interests

The authors declare that they have no known competing financial interests or personal relationships that could have appeared to influence the work reported in this paper.

Data availability

The data supporting this article have been included as part of the Supplementary Information.

References

[1] L.-L. Zhang, K. Tian, Z.-H. Tang, et al., Phytochemistry and Pharmacology of Carthamus tinctorius L, Am J Chin Med. 44 (2016) 197-226 https://doi.org/10.1142/S0192415X16500130.

[2] M. Ruyvaran, A. Zamani, A. Mohamadian, et al., Safflower (Carthamus tinctorius L.) oil could improve abdominal obesity, blood pressure, and insulin resistance in patients with metabolic syndrome: A randomized, double-blind, placebo-controlled clinical trial, Journal of Ethnopharmacology. 282 (2022) 114590 https://doi.org/10.1016/j.jep.2021.114590.

[3] X. Zhang, C. Shao, L. Jin, et al., Optimized Separation of Carthamin from Safflower by Macroporous Adsorption Resins and Its Protective Effects on PC12 Cells Injured by OGD/R via Nrf2 Signaling Pathway, J Agric Food Chem. 71 (2023) 18986-18998 https://doi.org/10.1021/acs.jafc.3c05285.

[4] Z. Zhang, C. Hu, F. Dai, et al., Mechanisms and status of research on the protective effects of traditional Chinese medicine against ischemic brain injury, Traditional Medicine Research. 7 (2022) 9 https://doi.org/10.53388/tmr20211021250.

[5] L. Yu, Z. Jin, M. Li, et al., Protective potential of hydroxysafflor yellow A in cerebral ischemia and reperfusion injury: An overview of evidence from experimental studies, Front Pharmacol. 13 (2022) 1063035 https://doi.org/10.3389/fphar.2022.1063035.

[6] F. Zhao, P. Wang, Y. Jiao, et al., Hydroxysafflor Yellow A: A Systematical Review on Botanical Resources, Physicochemical Properties, Drug Delivery System, Pharmacokinetics, and Pharmacological Effects, Front Pharmacol. 11 (2020) 579332 https://doi.org/10.3389/fphar.2020.579332.

[7] I. Adamska, P. Biernacka, Bioactive Substances in Safflower Flowers and Their Applicability in Medicine and Health-Promoting Foods, International Journal of Food Science. 2021 (2021) 6657639 https://doi.org/10.1155/2021/6657639.

[8] S. Yang, G. Lian, ROS and diseases: role in metabolism and energy supply, Molecular and Cellular Biochemistry. 467 (2020) 1-12 https://doi.org/10.1007/s11010-019-03667-9.

[9] D.B. Zorov, M. Juhaszova, S.J. Sollott, Mitochondrial reactive oxygen species (ROS) and ROS-induced ROS release, Physiological Reviews. 94 (2014) 909-950 https://doi.org/10.1152/physrev.00026.2013.

[10] H. Zhu, S. Hu, Y. Li, et al., Interleukins and Ischemic Stroke, Frontiers In Immunology. 13 (2022) 828447 https://doi.org/10.3389/fimmu.2022.828447.

[11] F. Herpich, F. Rincon, Management of Acute Ischemic Stroke, Critical Care Medicine. 48 (2020) 1654-1663 https://doi.org/10.1097/CCM.0000000000004597.

[12] J.-L. Yang, S. Mukda, S.-D. Chen, Diverse roles of mitochondria in ischemic stroke, Redox Biol. 16 (2018) 263-275 https://doi.org/10.1016/j.redox.2018.03.002.

[13] Z. Mao, L. Tian, J. Liu, et al., Ligustilide ameliorates hippocampal neuronal injury after cerebral ischemia reperfusion through activating PINK1/Parkin-dependent mitophagy, Phytomedicine. 101 (2022) 154111 https://doi.org/10.1016/j.phymed.2022.154111.

[14] Y. Zhang, Y. He, M. Wu, et al., Rehmapicroside ameliorates cerebral ischemia-reperfusion injury via attenuating peroxynitrite-mediated mitophagy activation, Free Radic Biol Med. 160 (2020) 526-539 https://doi.org/10.1016/j.freeradbiomed.2020.06.034.

[15] C. Holze, C. Michaudel, C. Mackowiak, et al., Oxeiptosis, a ROS-induced caspase-independent apoptosis-like cell-death pathway, Nature Immunology. 19 (2018) 130-140 https://doi.org/10.1038/s41590-017-0013-y.

[16] P. Scaturro, A. Pichlmair, Oxeiptosis-a cell death pathway to mitigate damage caused by radicals, Cell Death and Differentiation. 25 (2018) 1191-1193 https://doi.org/10.1038/s41418-018-0134-3.

[17] P. Scaturro, A. Pichlmair, Oxeiptosis: a discreet way to respond to radicals, Current Opinion In Immunology. 56 (2019) 37-43 https://doi.org/10.1016/j.coi.2018.10.006.

[18] D. Tang, R. Kang, T.V. Berghe, et al., The molecular machinery of regulated cell death, Cell Research. 29 (2019) 347-364 https://doi.org/10.1038/s41422-019-0164-5.

[19] L. Su, J. Zhang, H. Gomez, et al., Mitochondria ROS and mitophagy in acute kidney injury, Autophagy. 19 (2023) 401-414 https://doi.org/10.1080/15548627.2022.2084862.

[20] W. Xie, T. Zhu, S. Zhang, et al., Protective effects of Gypenoside XVII against cerebral ischemia/reperfusion injury via SIRT1-FOXO3A- and Hif1a-BNIP3-mediated mitochondrial autophagy, Journal of Translational Medicine. 20 (2022) 622 https://doi.org/10.1186/s12967-022-03830-9.

[21] G. Ashrafi, T.L. Schwarz, The pathways of mitophagy for quality control and clearance of mitochondria, Cell Death and Differentiation. 20 (2013) 31-42 https://doi.org/10.1038/cdd.2012.81.

[22] L. Shen, Q. Gan, Y. Yang, et al., Mitophagy in Cerebral Ischemia and Ischemia/Reperfusion Injury, Frontiers In Aging Neuroscience. 13 (2021) 687246 https://doi.org/10.3389/fnagi.2021.687246.

[23] L. Zhang, L. Dai, D. Li, Mitophagy in neurological disorders, J Neuroinflammation. 18 (2021) 297 https://doi.org/10.1186/s12974-021-02334-5.

[24] C. Cai, Z. Guo, X. Chang, et al., Empagliflozin attenuates cardiac microvascular ischemia/reperfusion through activating the AMPKα1/ULK1/FUNDC1/mitophagy pathway, Redox Biol. 52 (2022) 102288 https://doi.org/10.1016/j.redox.2022.102288.

[25] T. Tang, L.-B. Hu, C. Ding, et al., Src inhibition rescues FUNDC1-mediated neuronal mitophagy in ischaemic stroke, Stroke and Vascular Neurology. (2023) https://doi.org/10.1136/svn-2023-002606.

[26] B. Yu, J. Ma, J. Li, et al., Mitochondrial phosphatase PGAM5 modulates cellular senescence by regulating mitochondrial dynamics, Nature Communications. 11 (2020) 2549 https://doi.org/10.1038/s41467-020-16312-7.

[27] H. Zhu, Y. Tan, W. Du, et al., Phosphoglycerate mutase 5 exacerbates cardiac ischemia-reperfusion injury through disrupting mitochondrial quality control, Redox Biol. 38 (2021) 101777 https://doi.org/10.1016/j.redox.2020.101777.

[28] A. Zeb, V. Choubey, R. Gupta, et al., A novel role of KEAP1/PGAM5 complex: ROS sensor for inducing mitophagy, Redox Biol. 48 (2021) 102186 https://doi.org/10.1016/j.redox.2021.102186.

[29] S. Xu, P. Huang, J. Yang, et al., Calycosin alleviates cerebral ischemia/reperfusion injury by repressing autophagy via STAT3/FOXO3a signaling pathway, Phytomedicine. 115 (2023) 154845 https://doi.org/10.1016/j.phymed.2023.154845.

[30] Y. Fangma, H. Zhou, C. Shao, et al., Hydroxysafflor Yellow A and Anhydrosafflor Yellow B Protect Against Cerebral Ischemia/Reperfusion Injury by Attenuating Oxidative Stress and Apoptosis the Silent Information Regulator 1 Signaling Pathway, Front Pharmacol. 12 (2021) 739864 https://doi.org/10.3389/fphar.2021.739864.

[31] Y. Chen, W. He, H. Wei, et al., Srs11-92, a ferrostatin-1 analog, improves oxidative stress and neuroinflammation via Nrf2 signal following cerebral ischemia/reperfusion injury, CNS Neuroscience & Therapeutics. 29 (2023) 1667-1677 https://doi.org/10.1111/cns.14130.

[32] E.Z. Longa, P.R. Weinstein, S. Carlson, et al., Reversible middle cerebral artery occlusion without craniectomy in rats, Stroke. 20 (1989) 84-91 https://doi.org/10.1161/01.str.20.1.84.

[33] R. Dang, M. Wang, X. Li, et al., Edaravone ameliorates depressive and anxiety-like behaviors via Sirt1/Nrf2/HO-1/Gpx4 pathway, J Neuroinflammation. 19 (2022) 41 https://doi.org/10.1186/s12974-022-02400-6.

[34] G. Chen, C. Li, L. Zhang, et al., Hydroxysafflor yellow A and anhydrosafflor yellow B alleviate ferroptosis and parthanatos in PC12 cells injured by OGD/R, Free Radic Biol Med. 179 (2022) 1-10 https://doi.org/10.1016/j.freeradbiomed.2021.12.262.

[35] A. Liu, J. Hu, T.-S. Yeh, et al., Neuroprotective Strategies for Stroke by Natural Products: Advances and Perspectives, Current Neuropharmacology. 21 (2023) 2283-2309 https://doi.org/10.2174/1570159X21666230717144752.

[36] T. Zhu, L. Wang, L.-P. Wang, et al., Therapeutic targets of neuroprotection and neurorestoration in ischemic stroke: Applications for natural compounds from medicinal herbs, Biomed Pharmacother. 148 (2022) 112719 https://doi.org/10.1016/j.biopha.2022.112719.

[37] T. Tao, M. Liu, M. Chen, et al., Natural medicine in neuroprotection for ischemic stroke: Challenges and prospective, Pharmacology & Therapeutics. 216 (2020) 107695 https://doi.org/10.1016/j.pharmthera.2020.107695.

[38] H. Guo, L. Zhu, P. Tang, et al., Carthamin yellow improves cerebral ischemia-reperfusion injury by attenuating inflammation and ferroptosis in rats, Int J Mol Med. 47 (2021) https://doi.org/10.3892/ijmm.2021.4885.

[39] Y. Sun, D.-P. Xu, Z. Qin, et al., Protective cerebrovascular effects of hydroxysafflor yellow A (HSYA) on ischemic stroke, European Journal of Pharmacology. 818 (2018) 604-609 https://doi.org/10.1016/j.ejphar.2017.11.033.

[40] X. Zeng, Y.-D. Zhang, R.-Y. Ma, et al., Activated Drp1 regulates p62-mediated autophagic flux and aggravates inflammation in cerebral ischemia-reperfusion via the ROS-RIP1/RIP3-exosome axis, Mil Med Res. 9 (2022) 25 https://doi.org/10.1186/s40779-022-00383-2.

[41] E.G. Knox, M.R. Aburto, G. Clarke, et al., The blood-brain barrier in aging and neurodegeneration, Molecular Psychiatry. 27 (2022) 2659-2673 https://doi.org/10.1038/s41380-022-01511-z.

[42] Y. Cai, E. Yang, X. Yao, et al., FUNDC1-dependent mitophagy induced by tPA protects neurons against cerebral ischemia-reperfusion injury, Redox Biol. 38 (2021) 101792 https://doi.org/10.1016/j.redox.2020.101792.

[43] M. Lin, R. Hua, J. Ma, et al., Bisphenol A promotes autophagy in ovarian granulosa cells by inducing AMPK/mTOR/ULK1 signalling pathway, Environment International. 147 (2021) 106298 https://doi.org/10.1016/j.envint.2020.106298.

[44] W. Tian, M. Zhu, Y. Zhou, et al., Electroacupuncture Pretreatment Alleviates Cerebral Ischemia-Reperfusion Injury by Regulating Mitophagy via mTOR-ULK1/FUNDC1 Axis in Rats, Journal of Stroke and Cerebrovascular Diseases : the Official Journal of National Stroke Association. 31 (2022) 106202 https://doi.org/10.1016/j.jstrokecerebrovasdis.2021.106202.

[45] Y. Xiao, W. Chen, Z. Zhong, et al., Electroacupuncture preconditioning attenuates myocardial ischemia-reperfusion injury by inhibiting mitophagy mediated by the mTORC1-ULK1-FUNDC1 pathway, Biomed Pharmacother. 127 (2020) 110148 https://doi.org/10.1016/j.biopha.2020.110148